Comparison of Charge Models for Fixed-Charge Force Fields: Small-Molecule Hydration Free Energies in Explicit Solvent

David L. Mobley,*,† Élise Dumont,§ John D. Chodera,‡ and Ken A. Dill†

Department of Pharmaceutical Chemistry and Graduate Group in Biophysics, University of California at San Francisco, San Francisco, California 94143, and Laboratoire de Chimie Théorique, Centre National de la Recherche Scientifique UMR 7616, Université Pierre et Marie Curie-CNRS, Box 137, 4 Place Jussieu, 75252 Paris Cedex 05, France

Received: October 13, 2006; In Final Form: December 1, 2006

In molecular simulations with fixed-charge force fields, the choice of partial atomic charges influences numerous computed physical properties, including binding free energies. Many molecular mechanics force fields specify how nonbonded parameters should be determined, but various choices are often available for how these charges are to be determined for arbitrary small molecules. Here, we compute hydration free energies for a set of 44 small, neutral molecules in two different explicit water models (TIP3P and TIP4P-Ew) to examine the influence of charge model on agreement with experiment. Using the AMBER GAFF force field for nonbonded parameters, we test several different methods for obtaining partial atomic charges, including two fast methods exploiting semiempirical quantum calculations and methods deriving charges from the electrostatic potentials computed with several different levels of ab initio quantum calculations with and without a continuum reaction field treatment of solvent. We find that the best charge sets give a root-mean-square error from experiment of roughly 1 kcal/mol. Surprisingly, agreement with experimental hydration free energies does not increase substantially with increasing level of quantum theory, even when the quantum calculations are performed with a reaction field treatment to better model the aqueous phase. We also find that the semiempirical AM1-BCC method for computing charges works almost as well as any of the more computationally expensive ab initio methods and that the root-mean-square error reported here is similar to that for implicit solvent models reported in the literature. Further, we find that the discrepancy with experimental hydration free energies grows substantially with the polarity of the compound, as does its variation across theory levels.

I. Introduction

The hydration (or aqueous solvation) of chemical groups plays a critical role in almost all important biochemical processes, including protein folding, the formation of membranes, ligand binding, biomolecular interactions, and mixture properties. Proper accounting of hydration is also important for drug design, since the binding of small molecules to proteins causes desolvation of part or all of both the protein binding site and the small molecule. Because of the critical importance of desolvation in binding processes, some physics-based docking and rescoring packages now include desolvation corrections for both the small molecule and the binding site.[1−5] Inclusion of this correction improves the correlation of docking scores with experimental binding free energies and aids in eliminating molecules with inappropriate charge states from the set of potential high-affinity inhibitors.[1,4] Without these corrections, highly charged ligands do not experience a desolvation penalty when transferred from solvent to the (potentially) low-dielectric environment of the binding site and hence can be (incorrectly) preferentially scored in charged binding sites,[1] at least when using physics-based scoring functions.

Hydration free energies can now be computed very precisely using alchemical absolute free energy methods.[6,7] Their accuracy, however, is sensitive to a number of force field parameters, especially the partial atomic charges and Lennard-Jones parameters, as well as the choice of water model.[7] A number of general force fields, with parameters for arbitrary small druglike molecules, have recently been developed, including the general AMBER force field (GAFF),[8] but these typically only specify bonded and Lennard-Jones parameters; there are no widely accepted standards specifying how partial charges should be determined for arbitrary small molecules. For example, the popular AMBER 1994 and AMBER 1996 force fields have charge derived based on fitting of the electrostatic potential from self-consistent field (SCF) 6-31G* calculations, after which Lennard-Jones parameters were fit.[9] CHARMM 22 charges, however, come from the fitting of solute−water dimer energetics from SCF/6-31G* calculations, after which Lennard-Jones parameters were fit. GROMOS and OPLS have traditionally derived charge and Lennard-Jones parameters from fitting of properties of pure liquids and transfer free energies rather than from quantum calculations.[9] Furthermore, the ANTECHAMBER package[10] for parametrizing small molecules with GAFF provides no less than seven methods for computing partial charges as well as methods to fit charges given input from quantum mechanical calculations.

Recently, much effort has focused on (1) estimating hydration free energies directly from semiempirical quantum mechanical methods with continuum solvent models (e.g., refs 11 and 12),

* Author to whom correspondence should be addressed. E-mail: dmobley@maxwell.compbio.ucsf.edu.

† Department of Pharmaceutical Chemistry, University of California at San Francisco.

‡ Graduate Group in Biophysics, University of California at San Francisco.

§ Université Pierre et Marie Curie.

10.1021/jp0667442 CCC: $37.00
Published on Web 02/10/2007 PAGE EST: 12.6

(2) applying better levels of quantum theory to parametrizing force fields for molecular simulation,[13,14] and (3) computing precise hydration free energies of amino acid side-chain analogues with various force fields.[6,7,15,16] But there has been little or no recent work that combines charges derived from higher-level quantum calculations with explicit solvent and the latest free energy methods to calculate hydration free energies for a diverse set of small molecules. This can provide both a benchmark of the accuracy of current force fields and an assessment of the accuracy that can be expected from binding free energy calculations. Here, we perform exactly this test, in an effort to determine the best approach for obtaining these partial charges.

While there is likely a fundamental limit to the accuracy of fixed-charge force fields due to the neglect of polarizability and the adoption of simple functional forms to represent atomic interactions, it is worthwhile to explore how much agreement can be expected of the current generation of molecular mechanics force fields. Hydration or transfer free energies provide a reasonable benchmark, as inaccuracies in hydration free energies will probably lead to inaccuracies in binding free energies, barring fortuitous cancellation of errors.

Here, we use the general AMBER force field (GAFF) parameter set[8] and compare different methods of obtaining partial charges for small molecules. We test charge determination methods including population-analysis methods based on semiempirical quantum calculations (AM1-CM2[17] and AM1-BCC[18]) and restrained electrostatic potential (RESP) fitting[19] applied to a number of ab initio methods (HF/6-31G*, B3LYP/6-31G*, B3LYP/cc-pVTZ, and MP2/cc-pVTZ, as discussed in section II) both with and without a reaction field treatment of the solvent. For each partial charge set, we consider two different explicit water models (TIP3P[20] and TIP4P-Ew[21]).

II. Methods

A. Selection of the Small-Molecule Test Set. In this study, we consider a set of 44 uncharged small organic molecules for which experimental hydration free energies are known (Figure 1). These molecules contain representative chemical moieties commonly encountered in libraries of druglike molecules, including aliphatic and aromatic compounds, alkanes, alkenes, alcohols, amines, halides, thiols, esters, and amides. This set also contains a complete set of neutral amino acid side-chain analogues to allow comparison with a previous study.[6]

It is worth noting that there are a number of complications associated with calculating, or experimentally measuring, hydration free energies of charged compounds. On the computational side, these are only beginning to be resolved.[22] Therefore, we have deliberately included only neutral molecules in our test set.

B. Quantum Chemical Calculations. To obtain atomic partial charges through electrostatic potential fitting methods, the molecular electron density must be computed using some level of either semiempirical, Hartree−Fock, density functional theory (DFT), or post-Hartree−Fock methods. The Gaussian 03 series of programs was used throughout this work for quantum chemical calculations.[23]

First, to produce a reasonable electron density capable of accurately representing the ground state electronic distribution of the molecule, molecular geometries (initially extracted from mol2 files in the Bordner et al. set[24,25]) must be optimized with an appropriate level of quantum theory to produce a conformation mostly free of strain. Here, geometry optimizations were performed on all molecules with Becke's three-parameter density functional hybrid method[26] combined with the Lee, Yang, and Parr gradient-corrected correlation functional (B3LYP)[27] with the correlation consistent polarized triple-ζ (cc-pVTZ, also abbreviated TZ) basis set of Dunning and co-workers.[28] This basis set includes 4s, 3p, 2d, and 1f orbital functions for heavy atoms and 3s, 2p, and 1d for hydrogens. The corresponding level of calculation, B3LYP/cc-pVTZ, generally performs well for geometry optimization without requiring long calculation times.[29]

Single-point calculations were then performed at three different levels of theory: ab initio Hartree−Fock (HF) SCF, DFT with the B3LYP functional as described above, and second-order Møller−Plesset perturbation theory (MP2).[30] For each, we used one or two basis set(s), namely, the standard 6-31G* Pople basis set[31] and cc-pVTZ. In total, four combinations of theory and basis set were employed: SCF/6-31G*, B3LYP/6-31G*, B3LYP/cc-pVTZ, and MP2/cc-pVTZ.

The reasoning behind these choices was fairly simple. SCF/6-31G* has traditionally been employed for determining partial charges for peptides for several molecular mechanics force fields, due to its modest computational cost and tendency to overestimate gas-phase dipole moments, which has been suggested as a potential way of accounting for the three-body interactions neglected in nonpolarizable force fields.[9,32] The description of the AMBER charge fitting philosophy in the AMBER8 manual[32] states:

> The 6-31G* basis set tends to result in dipole moments which are 10−20% larger than gas phase. This behavior is desirable for deriving charges to be used for condensed phase simulations within an effective two-body additive model, where polarization is being represented implicitly. In other words a molecule is expected to be more polarized in condensed phase vs gas phase due to many body interactions, so we "pre-polarize" the charges.

However, the availability of more powerful computers now permits the use of more sophisticated methods to compute more accurate electrostatic potentials and, hopefully, superior partial charges.[13,33] Indeed, higher levels of theory have recently been employed in reparameterizing torsion terms for both CHARMM[34] and AMBER.[13]

While full configuration interaction (CI) calculations are still too expensive to allow large numbers of molecules to be treated, DFT and perturbation theory are both inexpensive enough to apply to small molecules on a wide scale, and we consider both here. Therefore, in addition to SCF/6-31G*, we used the common DFT/B3LYP functional and the MP2 method.

All ab initio calculations were also performed with and without a self-consistent reaction field (SCRF),[35] intended to mimic the solvated environment and obtain a polarized charge distribution suitable for simulations in the aqueous phase. We employed the polarizable continuum model (PCM)[35] with an external dielectric constant of 78.39. The integral equation formalism (IEF) method for polarizable continuum models was used, with the United Atom Topological Model (UA0) for the cavity, using the default parameters of Gaussian 03. Several methods for specifying the molecular cavity were tested for phenol and toluene, where it was determined that partial charges obtained after RESP fits differed by less than 1% when explicit hydrogens were used to compute the cavity; therefore we considered only this single approach for the remainder of our calculations (data not shown).

RESP[19] charges were obtained from the electrostatic potential using the ANTECHAMBER package (AMBER 8 version).[10]

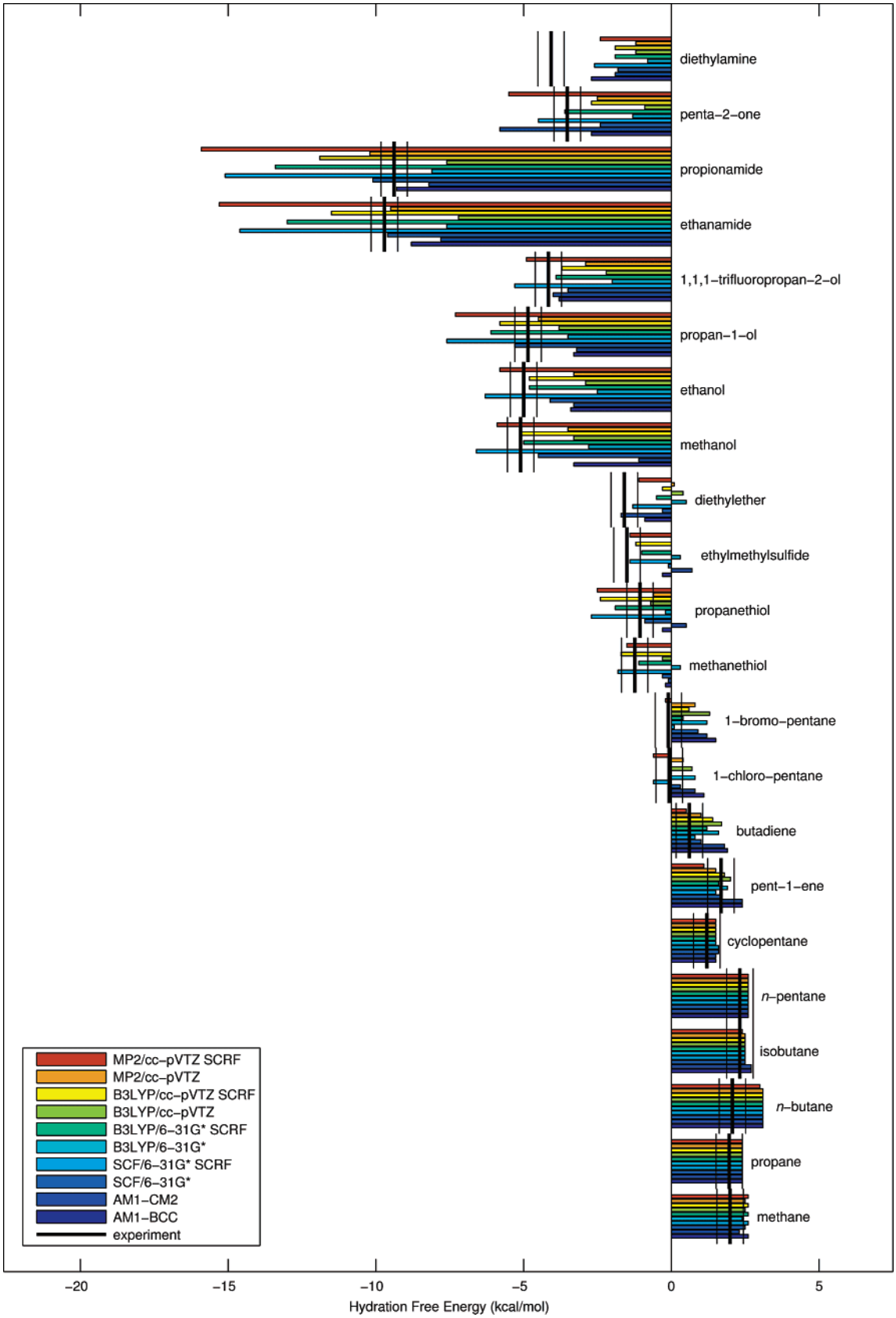

Figure 1. Experimental and calculated free energies in TIP3P: Part 1. Experimental values are shown as a thick black vertical line; estimated experimental uncertainties are shown as thin vertical lines. Estimated uncertainties in calculated free energies are comparable to the experimental uncertainties. Part 2 of the test set is found in Figure 2.

RESP can be used to fit partial charges to electrostatic potentials computed from either a single conformation (single conformer fit) or a number of different conformations (multiconformer fit). One weakness of charges derived from fitting the electrostatic potential is the sometimes strong dependence on the molecular configuration used to compute the electrostatic potential.[36] Some have proposed including multiple conformations in the fitting procedure to mitigate this effect and derive an optimal charge

set that is suitable for multiple conformations.[37,38] Here, as our test set consists primarily of molecules with no or few rotatable bonds and significant geometry dependence of the electrostatic potential is not expected, we consider only single conformer fits to the optimized geometries obtained as described above. To ensure that this assumption was reasonable, we computed partial charges after performing QM calculations for a variety of different torsional angles for two small molecules in our set containing a rotatable bond, phenol and toluene. We find that the resulting hydration free energies vary only very slightly with the torsional angle (by approximately 0.05 kcal/mol, within our statistical uncertainty), and hence we do not further examine the issue of multiconformer fits for the remainder of this work. This issue, however, should be reexamined for molecules containing numerous rotatable bonds connecting strong polar or charged functionalities.

C. Semiempirical Charges. The same unoptimized mol2 files that were used as inputs for Gaussian geometry optimization above were used as inputs into the ANTECHAMBER package and used to compute AM1-BCC[18] charges. AM1-CM2 charges were computed with AMSOL, version 6.5.3,[39] on the same set of geometries. This approach is commonly employed in some docking calculations (e.g., in ref 1).

D. Small-Molecule Parametrization. General AMBER force field[8] parameters were assigned for all molecules in this study using the AMBER 8 version of the ANTECHAMBER package.[10] SYBYL mol2 files from the AMBER 8[40] ANTECHAMBER package were read into the AMBER 8 utility TLEAP and used to generate AMBER topology and coordinate files,[60] with coordinates taken from the Bordner et al. set.[24,25] These were converted to GROMACS topology and coordinate files using a Perl script that can be obtained from the Pande group.[41]

E. Alchemical Free Energy Calculations. Hydration free energies were computed using a thermodynamic cycle in which all electrostatic interactions of the solute were annihilated and Lennard-Jones interactions with the solvent environment were decoupled, bringing the solute to an uncharged vacuum reference state. Electrostatic interactions were then restored in vacuum to complete a thermodynamic cycle equivalent to transferring the molecule from solvent to vacuum. More rigorously, the desired hydration free energy is given by

$$\mathrm{M_{aq}} \xrightarrow{-\Delta G_{\mathrm{hyd}}} \mathrm{M_{gas}} \tag{1}$$

Here, $\mathrm{M_{aq}}$ denotes the molecule in water, and $\mathrm{M_{gas}}$ the molecule in the gas phase.

We compute ΔG_{hyd} alchemically, using the series of transformations

$$\mathrm{M_{aq}} \xrightarrow{\Delta G_{\mathrm{elec,aq}}} \mathrm{M_{aq,C}} \xrightarrow{\Delta G_{\mathrm{LJ,aq}}} \mathrm{M_{aq,C,L}} \tag{2}$$

$$= \mathrm{M_{gas,C,L}} = \mathrm{M_{gas,C}} \xrightarrow{-\Delta G_{\mathrm{elec,gas}}} \mathrm{M_{gas}} \tag{3}$$

Here, $\mathrm{M_{aq,C}}$ denotes the uncharged molecule in solvent, $\mathrm{M_{aq,C,L}}$ the uncharged molecule in solvent with its Lennard-Jones interactions with the solvent eliminated, and $\mathrm{M_{gas,C,L}}$ the uncharged molecule in the gas phase with with no Lennard-Jones interactions with its environment, which is equivalent to having the uncharged molecule in the gas phase interacting with its environment ($\mathrm{M_{gas,C}}$). The cycle is completed by restoring the electrostatic interactions in vacuum. Thus

$$-\Delta G_{\mathrm{hyd}} = \Delta G_{\mathrm{elec,aq}} + \Delta G_{\mathrm{LJ,aq}} - \Delta G_{\mathrm{elec,gas}} \tag{4}$$

This cycle is very similar to that used by Shirts and collaborators[6,7] in computing hydration free energies of neutral amino acid side-chain analogues, except all electrostatic interactions of the solute are eliminated entirely (annihilation) rather than only those electrostatic interactions between the molecule and the environment (as in decoupling). This difference necessitates the use of an additional vacuum calculation in which the charges are restored, as is done here, but does not require the source code modifications of GROMACS needed for the method used by Shirts and collaborators.

While this complete thermodynamic cycle could be computed for every partial charge set considered, it is more efficient to perform the entire calculation only once for each molecule, using a reference charge set, and simply add an additional step in which the partial charges are transformed from the reference charge set to the charge set of interest at both the $\mathrm{M_{aq}}$ and $\mathrm{M_{gas}}$ endpoints. The hydration free energy for a charge set of interest ΔG_{hyd}, in terms of the hydration free energy for the reference charge set $\Delta G_{\mathrm{hyd}}^{\mathrm{ref}}$, is given by

$$\Delta G_{\mathrm{hyd}} = \Delta G_{\mathrm{ref\rightarrow new,aq}} + \Delta G_{\mathrm{hyd}}^{\mathrm{ref}} - \Delta G_{\mathrm{ref\rightarrow new,gas}} \tag{5}$$

This method was adopted in this work, with the AM1-BCC charge set chosen as the reference set. The free energy of transforming the charges was computed by a series of alchemical intermediates between the two charge states, whose potential energy $U(\lambda)$ was defined as a linear combination of the potential energies for the reference and desired charge states

$$U(\lambda) = (1 - \lambda)U_0 + \lambda U_1 \tag{6}$$

where U_0 is the potential energy with the original (reference) charges, U_1 is the potential energy with the new charges, and λ a coupling parameter that runs from 0 to 1.

Free energy differences for each of the steps were computed using the Bennett acceptance ratio (BAR) method,[42,43] a type of free energy perturbation (FEP).[44] The BAR approach allows free energy differences between neighboring λ-values to be computed in a way that optimally uses all data from these two simulations, at the expense of requiring recomputation of the energies from each stored configuration at both neighboring λ-values.[43] We use the postprocessing approach described previously[45] for calculating the work values needed for the BAR method. All simulations were performed with GROMACS,[46,47] version 3.3, with a bug fix applied to the particle mesh Ewald (PME) section of the code. (The bug fix has been incorporated into GROMACS 3.3.1.)

After preparation of GROMACS topology and coordinate files using the conversion script described above, molecules were placed in a dodecahedral simulation box, with the size of the box determined such that the minimum distance from any atom in the molecule to the box edge was 12 Å. For solvated simulations, the remainder of the box was then filled with water molecules (TIP3P[20] or TIP4P-Ew[21]). The number of water molecules was typically 500−1000 depending on the size of the solute.

After preparation of the solvated system, separate calculations were performed from the same starting structure at each λ value for annihilating electrostatics and decoupling Lennard-Jones interactions in solvent and for restoring the electrostatic interactions in vacuum. Simulations at all alchemical intermediate states were conducted in parallel. All simulations in which electrostatics were modified were conducted at $\lambda = \{0,0.25,0.5,0.75,1\}$; Lennard-Jones decoupling simulations were

conducted at $\lambda = \{0,0.05,0.1,0.2,0.3,0.4,0.5,0.6,0.65,0.7,0.75,0.8,0.85,0.9,0.95,1\}$, using soft core potentials as in previous work.[45]

Short-range interactions were evaluated using a neighbor list of 10 Å updated every 10 steps, and Lennard-Jones interactions were switched off smoothly between 8 and 9 Å. A long-range analytical dispersion correction[6] was applied to the energy and pressure to account for the truncation of these interactions. Electrostatic interactions were evaluated with a real-space cutoff of 9 Å, and the PME method[48] was used for the long-range component of these interactions. We employed a PME spline order of 6, a Fourier spacing of 1.0 Å, and a relative tolerance between long- and short-range energies of 10^{-6}. In all of our calculations, integration was performed with Langevin dynamics,[49] with a reference temperature of 300 K and a weak frictional constant of 10 ps^{-1}, to avoid ergodicity and thermalization problems when the molecule is fully decoupled from the rest of the system. Vacuum calculations used the same parameters, except the electrostatics cutoff and neighbor list were made large enough to include the entire molecule, and periodicity was turned off.

Prior to simulation at each λ value, the system was first minimized and equilibrated. Up to 5000 steps of L-BFGS minimization[50] were performed, followed by 500 steps of steepest-descent minimization, as the L-BFGS minimizer would occasionally terminate early. To equilibrate the system, velocities were first assigned from a Maxwell−Boltzmann distribution at 300 K, and thermostated molecular dynamics was run for 10 ps. This was followed by 100 ps of dynamics using the Langevin integrator with the volume adjusted by the Berendsen weak-coupling scheme[51] with a time constant of 0.5 ps, a reference pressure of 1.0 atm, and an isothermal compressibility of 4.5×10^{-5} bar. After equilibration, production simulations were conducted with a fixed simulation volume for 5 ns. All molecular dynamics simulations employed a leapfrog integrator with a time step of 2 fs, using LINCS[52] with an order of 12 to restrain all bonds to hydrogen.

Uncertainties were estimated using the block bootstrap method,[53] with block lengths determined by the statistical inefficiency g, computed as described elsewhere.[54,55] The standard deviation in the computed free energy over 40 bootstrap realizations provides an estimate of the statistical uncertainty over repeated hydration free energy calculations.[61] Our calculations were sufficiently long that estimated uncertainties for all computed free energies were less than 0.1 kcal/mol. Free energies reported here are therefore presented with one decimal place of precision, and the computed uncertainties are omitted to save space.

To assess agreement with experimental data, it is necessary to also consider the uncertainties in the experimental measurements. Unfortunately, these uncertainties are often not reported. However, several studies have surveyed measurements of hydration free energies of the same molecules reported by different experimental groups. The observed variation in measurements, if obviously problematic measurements are excluded, is typically in the range of 0.01−0.1 kcal/mol.[6,56] Further, for the test set used here, experimental uncertainties were suggested to be typically around 0.2 kcal/mol but sometimes larger.[57] Thus, the experimental uncertainty is probably on the same order of magnitude as the computational uncertainty in this work.

F. Polarization Corrections. Experimental hydration free energies include a contribution—the polarization of the electronic wave function in response to transfer from the gas phase to the condensed phase—that is a purely quantum mechanical phenomenon. This polarization energy is always positive, reflecting the cost of deforming the electronic wave function from the gas-phase ground state to some average wave function appropriate for the aqueous phase, before the favorable electrostatic interactions with the polarized environment are included. Additionally, the charge distributions of the molecule in the gas phase and in the aqueous phase differ, something not reflected in our calculations here, which assume a fixed set of partial charges.

There is currently no consensus on how to properly correct computed free energies for this polarization energy, so we considered the following two alternatives. In one, discussed by Chipot,[15] the small molecule is treated at the same level of quantum theory with and without continuum solvation. The polarization energy is then the difference in the self-energy of the molecule with and without polarization by the environment. This contribution is always unfavorable and represents a correction that can be applied to the hydration free energies computed from charges obtained with the continuum solvent treatment. This correction was computed for each level of theory.

Alternatively, experimental hydration free energies can be regarded as including two contributions: (1) the free energy of polarizing the charge distribution in vacuum to the charge distribution appropriate for water and (2) the free energy of transferring a prepolarized molecule from vacuum to water. Our alchemical free energy calculations compute only quantity 2. To compare with experiment, we can add an estimate of quantity 1 to the computed hydration free energies, using some suitably high level of quantum theory and a continuum solvent treatment, here taken to be B3LYP/cc-pVTZ with and without a SCRF.

III. Results and Discussion

Computed hydration free energies are shown graphically for TIP3P in Figures 1, 2, and 3. Figures depicting hydration free energies for TIP4P-Ew can be found in the Supporting Information as well as can a table containing all of the computed hydration free energies for both water models. Statistics are available in Table 1. We present tests of these corrections in section III.J; otherwise, they were not included in computed hydration free energies.

A. Effect of the Solvent Model. First, we find that the TIP3P water model generally gives better hydration free energies than TIP4P-Ew, which has an average error from 0.2 to 0.8 kcal/mol worse depending on the charge set (Table 1). This is somewhat surprising, since TIP4P-Ew has been parametrized for use with long-range Ewald electrostatics,[21] which we use here, while TIP3P has not, and has been shown to have superior bulk properties.[21] A similar observation was recently made by two other groups.[7,16] Part of the reason for this difference may be, as previously suggested,[7] that TIP4P-Ew was optimized to better reproduce pure water properties, which may actually make solvent−solute interactions less accurate when done in the absence of other concerns.

Although the TIP4P-Ew hydration free energies are slightly worse than those computed using TIP3P, trends are qualitatively very similar, so for the remainder of this work we focus mostly on TIP3P results, although additional data and plots for TIP4P-Ew are available in the Supporting Information.

B. Comparison of Semiempirical and Ab Initio Methods. Second, we observe that the AM1-BCC charges reproduce experimental hydration free energies nearly as well as the best of the RESP charges (Table 1), despite the small computational cost of computing these charges compared to those obtained from the ab initio methods. None of the RESP-derived charge

TABLE 1: Statistics for Computed[a] Hydration Free Energies from This Study, Relative to Experimental Results[b]

				RESP ab initio charges							
					SCF/6-31G*		B3LYP/6-31G*		B3LYP/TZ		MP2/TZ
solute		AM1-BCC	AM1-CM2	SCF/6-31G*	SCRF	B3LYP/6-31G*	SCRF	B3LYP/TZ	SCRF	MP2/TZ	SCRF
TIP4P-Ew	AUE	1.24	1.55	1.27	2.43	2.03	1.65	1.93	1.45	1.46	2.46
	RMSE	1.51	2.27	1.58	3.69	2.40	2.53	2.32	1.96	1.79	3.97
	R^2	0.93	0.78	0.88	0.90	0.81	0.89	0.85	0.90	0.84	0.88
	slope	1.22	1.22	1.15	1.72	0.89	1.47	0.86	1.34	1.07	1.76
TIP3P	AUE	0.92	1.38	0.82	1.62	1.62	0.91	1.58	0.78	1.00	1.66
	RMSE	1.10	1.97	1.04	2.17	1.97	1.29	1.90	1.00	1.29	2.35
	R^2	0.94	0.75	0.94	0.96	0.92	0.95	0.94	0.95	0.91	0.94
	slope	1.03	1.04	0.98	1.39	0.79	1.21	0.79	1.13	0.93	1.40

[a] All computed free energies have a computed uncertainty (one standard deviation of the mean) of less than 0.1 kcal/mol. [b] Values are given in kcal/mol. We report average unsigned errors (AUEs), root-mean-square error (RMSEs), linear correlation coefficients (R^2), and the slope of this correlation between experimental and calculated hydration free energies. Experimental hydration free energies were taken from ref 57 and have an uncertainty of 0.2 kcal/mol. The full set of hydration free energies for both water models is available in the Supporting Information.

TABLE 2: Comparison of Hydration Free Energies with the TIP3P Water Model for 14 Different Side-Chain Analogues with Different Force Fields[a]

			this study						
			empirical	RESP			free energies from ref 7		
solute	amino acid	ΔG_{exp}	AM1-BCC	SCF/6-31G*	B3LYP/6-31G* SCRF	B3LYP/TZ SCRF	AMBER	CHARMM	OPLS
methane	Ala	1.99	2.6	2.5	2.6	2.6	2.57	2.44	2.31
propane	Val	1.96	2.4	2.4	2.4	2.4	2.69	2.52	2.59
n-butane	Ile	2.07	3.1	3.1	3.1	3.1	2.72	2.94	2.69
isobutane	Leu	2.32	2.7	2.5	2.5	2.5	2.84	2.67	2.73
methanol	Ser	−5.10	−3.3	−4.5	−5.0	−5.1	−4.37	−4.59	−4.36
ethanol	Thr	−5.00	−3.4	−6.3	−4.8	−4.8	−3.83	−4.22	−4.11
toluene	Phe	−0.80	−0.7	−2.2	−1.8	−1.3	0.10	0.09	−0.54
p-cresol	Tyr	−6.11	−5.4	−4.1	−5.9	−5.9	−4.23	−4.46	−5.25
methanethiol	Cys	−1.24	−0.2	−0.3	−1.1	−1.7	0.11	0.02	−1.59
ethylmethylsulfide	Met	−1.50	−0.3	−0.1	−1.0	−1.2	0.91	1.08	−1.27
ethanamide	Asn	−9.71	−8.8	−9.6	−13.0	−11.5	−7.80	−7.89	−8.53
propionamide	Gln	−9.38	−9.3	−10.1	−13.4	−11.5	−7.69	−7.51	−8.40
3-methylindole	Trp	−5.88	−6.5	−5.3	−6.9	−6.6	−4.88	−3.57	−4.44
4-methylimidazole	Hid/Hie	−10.27	−8.4	−8.2	−12.3	−11.5	−8.98	−9.27	−9.05
		AUE	0.89	0.96	1.06	0.70	1.20	1.21	0.80
		RMSE	0.92	0.96	1.01	0.81	1.08	1.08	0.88
		R^2	0.98	0.95	0.97	0.99	0.99	0.98	0.99
		slope	1.00	0.96	0.77	0.85	1.06	1.06	1.04

[a] Values are given in kcal/mol. We report average unsigned errors (AUEs), root-mean-square error (RMSEs), linear correlation coefficients (R^2), and the slopes of this correlation between experimental and calculated hydration free energies.

sets substantially outperform these charges (i.e., by more than 0.2 kcal/mol in average/root-mean-square error (RMSE); 0.2 kcal/mol is probably a reasonable criteria, since it represents a ballpark uncertainty in a typical experimental hydration free energy). The AM1-BCC charges therefore appear to be a reasonable choice, though as we discuss below ab initio charges may perform better for molecules containing certain chemical moieties. With AM1-BCC, there is a good linear correlation between calculated and experimental hydration free energies, with a slope near unity ($R^2 = 0.94$ with TIP3P, 0.93 with TIP4P-Ew). AM1-CM2 charges led to a greater discrepancy with experiment (an average unsigned error of 1.4 kcal/mol with TIP3P and more than 1.5 kcal/mol with TIP4P-Ew, as shown in Table 1). As noted elsewhere,[18] the empirical BCC correction applied to AM1-CM2 charges (to obtain AM1-BCC charges) substantially improves the agreement with experiment for some small molecules. Rizzo et al. recently observed similarly good performance of AM1-BCC charges in implicit solvent on a much larger test set.[25]

RESP charges derived from electrostatic potentials computed with SCF/6-31G* perform slightly better than AM1-BCC, which is not too surprising, since the empirical corrections used in AM1-BCC were parametrized to reproduce RESP SCF/6-31G* charges.[19] In view of the fact that RESP charges do seem to perform slightly better, one can legitimately wonder if higher-level ab initio calculations could improve agreement with experiment. However, our results show that only two sets of ab initio charges, SCF/6-31G* and B3LYP/cc-pVTZ with a SCRF correction, performed well compared to AM1-BCC.

C. Comparison with Previous Work and Other Force Fields. Our test set also includes neutral amino acid side-chain analogues, which have been recently examined by Shirts et al., who computed hydration free energies using parameters and charges derived from the published amino acid parameters for several force fields.[7] In Table 2, we compare our hydration free energies with those of Shirts et al. Here, we use the GAFF force field, a general version of the AMBER force field, so force field parameters are similar, but not identical, to those of the AMBER calculations in ref 7. We find that SCF/6-31G* calculations, as used to parametrize AMBER, give an RMSE (1.09) very comparable to their AMBER RMSE(1.08) but that both AM1-BCC and B3LYP/cc-pVTZ SCRF partial charges give substantially lower RMSEs (0.9 in both cases), comparable to those of the best of the force field that they tested, OPLS.

D. Variation across Charge Models. Figure 3 compares experimental and computed hydration free energies. We find

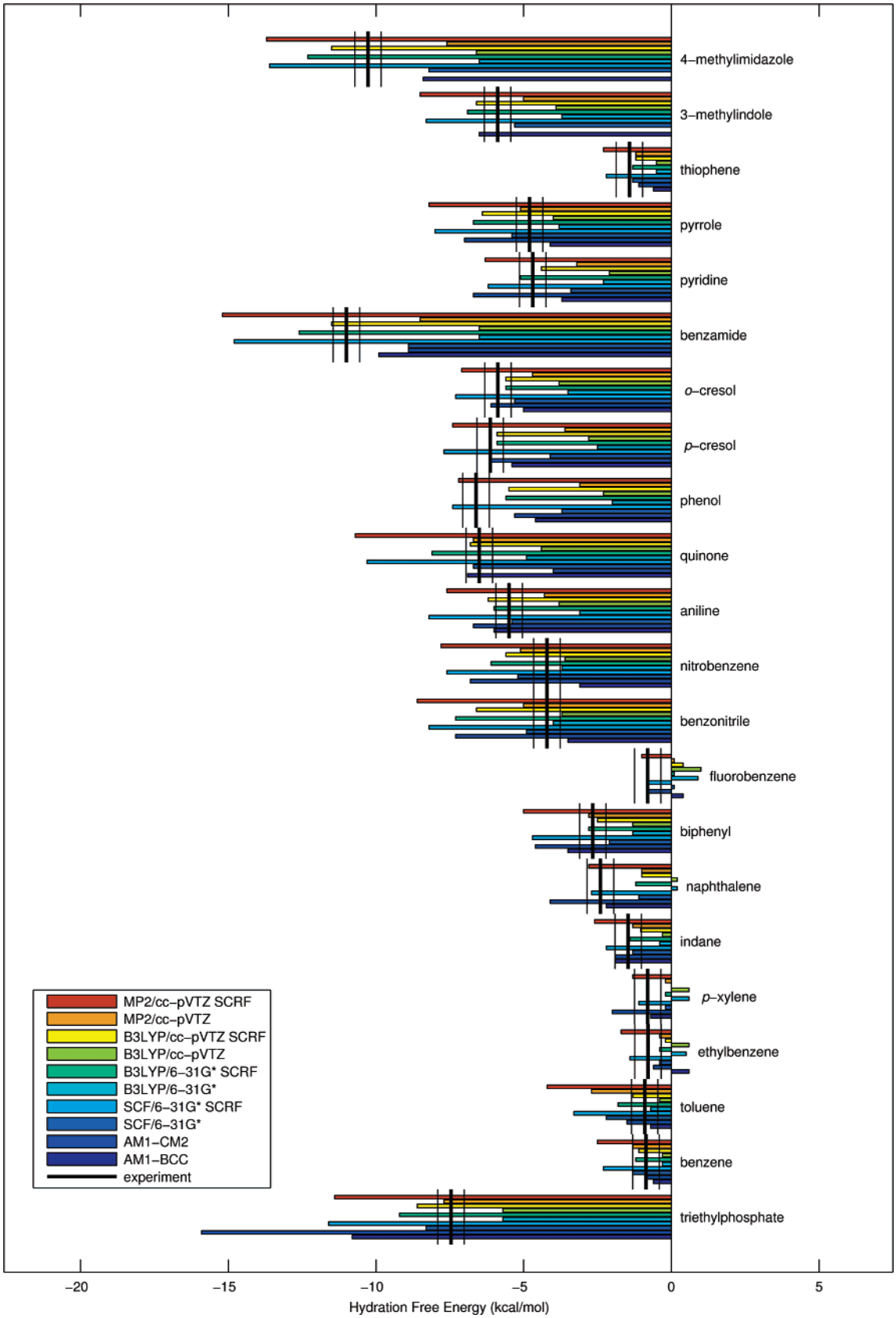

Figure 2. Experimental and calculated free energies in TIP3P: Part 2. Experimental values are shown as a thick black vertical line; estimated experimental uncertainties are shown as thin vertical lines. Estimated uncertainties in calculated free energies are comparable to the experimental uncertainties. Part 1 of the test set is found in Figure 1.

that greater polarity, which correlates with larger in magnitude (and more negative) hydration free energies, is also correlated with larger variance in the computed hydration free energies among the charge models tested. This is not surprising, since charges for apolar molecules will be small and hydration free energies are dominated by the other force field parameters (i.e., the Lennard-Jones parameters for the molecule and the parameters for water). It is interesting to note that computed hydration

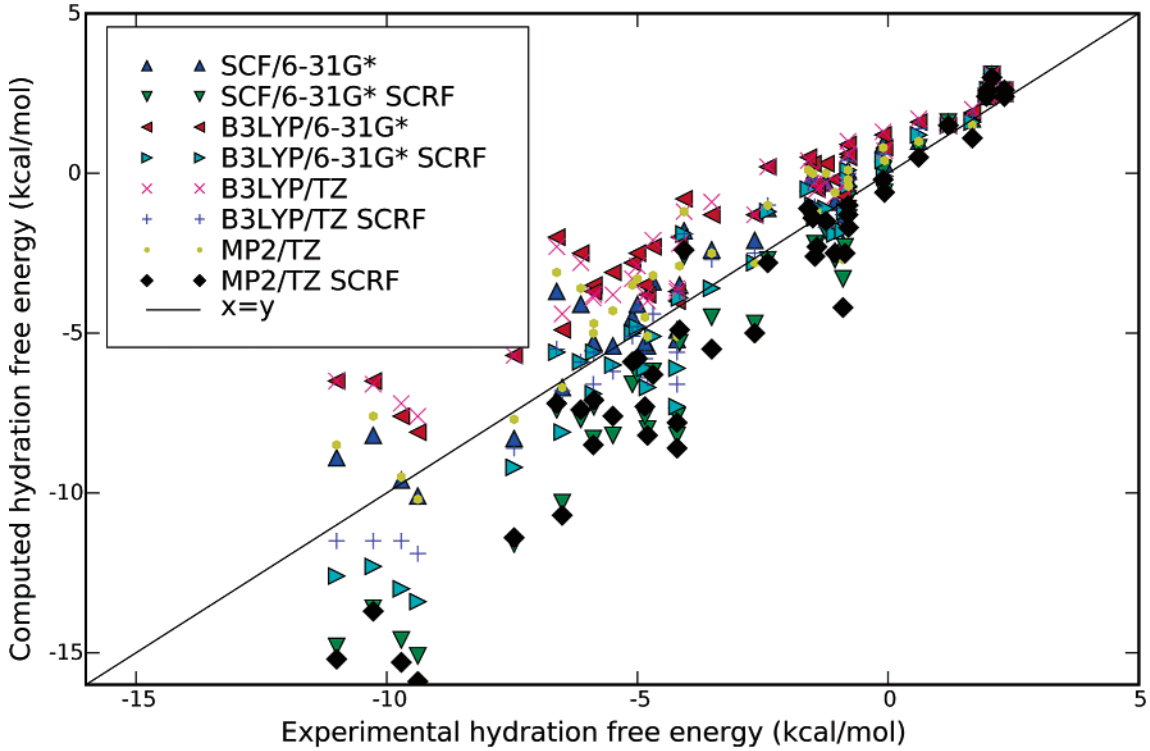

Figure 3. Comparison of experimental and computed hydration free energies in TIP3P for all levels of theory. Computed hydration free energies are compared with the experimental values for all of the molecules in the test set at each theory level in TIP3P water. A similar figure for TIP4P-Ew is available in the Supporting Information.

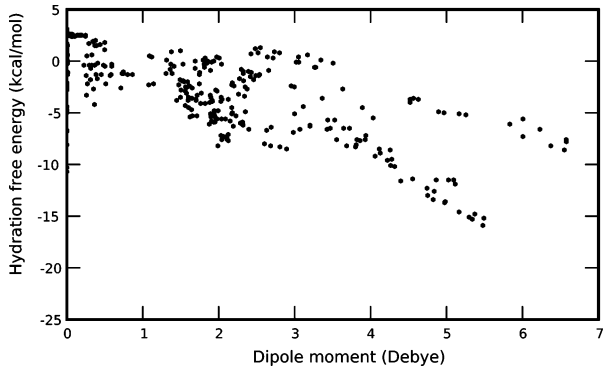

Figure 4. Correlation of the computed hydration free energy in TIP3P water with the RESP-derived dipole moment. The dipole moment was computed from the partial charges obtained by RESP fitting. All levels of theory are shown. The correlation coefficient, R^2, is 0.52; the slope is −0.8. There is one data point per molecule (44) per ab initio charge model (8) for a total of 352 data points. Additional figures for TIP4P-Ew and for just the electrostatic component of the hydration free energy are available in the Supporting Information.

free energies are reasonably well correlated with the dipole moment (Figure 4, $R^2 = 0.52$) and the dipole moment for a given molecule varies substantially across theory levels (Figure 6). (In the Supporting Information, we also provide similar details concerning the electrostatic components of the hydration free energies.) This may explain part of the substantial variation in hydration free energies across theory levels. However, in addition to the dipole moment, the RESP-derived partial charges can also differ significantly (Figure 5) among different charge sets. While the dipole moment dominates the electrostatics far from the molecule, hydrogen-bonding properties are likely to be more sensitive to the details of the charge distribution and may be significantly affected by this variation in partial charges. This also may be the source of some of the variation across charge sets.

E. Effect of the Reaction Field. As discussed in section II.B, the historical reason for deriving charges from SCF/6-31G* electrostatic potentials is that this particular choice overpolarizes the vacuum charges in a way that could be considered appropriate for condensed phase simulation, where the always-attractive three-body correlations could be accounted for in an average way. One might hope to achieve this same effect without relying on the deficiencies of the 6-31G* basis set by using a higher level of theory with a reaction field (SCRF) to mimic the polarizable environment. However, this does not seem to systematically improve the agreement with experiment. Computed free energies are better without SCRF for SCF and MP2, as charges derived from electrostatic potentials computed from quantum calculations with SCRF appear to overestimate the affinity for water. This is especially striking for very polar compounds, such as amides. Elsewhere, it has been suggested that an intermediate value for the exterior dielectric constant be used ($\epsilon = 4$, instead of the value for water, around 80, which was used here)[13] to improve agreement with experimental data. It is possible that this would allow tuning of the SCRF correction to improve agreement of hydration free energies with experimental results, but this would be an empirical correction, which seems rather unsatisfying. It would also need to be different for different charge models. However, SCRF does improve the agreement with experiment for the B3LYP calculations.

F. Comparison with Implicit Solvent. Rizzo et al. have recently computed hydration free energies for a larger set of molecules using several implicit solvent models.[25] We can compare our results with these implicit solvent results for the same molecules in Table 3. For the AM1-BCC and RESP-derived charges, our average unsigned discrepancy with experiment in TIP3P is approximately 0.4 kcal/mol less than the implicit (GB/SA) solvent error, while our average error in TIP4P-Ew is comparable. (Our comparison is with the data used to generate Table 3 of the work of Rizzo et al.[25]) Explicit solvent

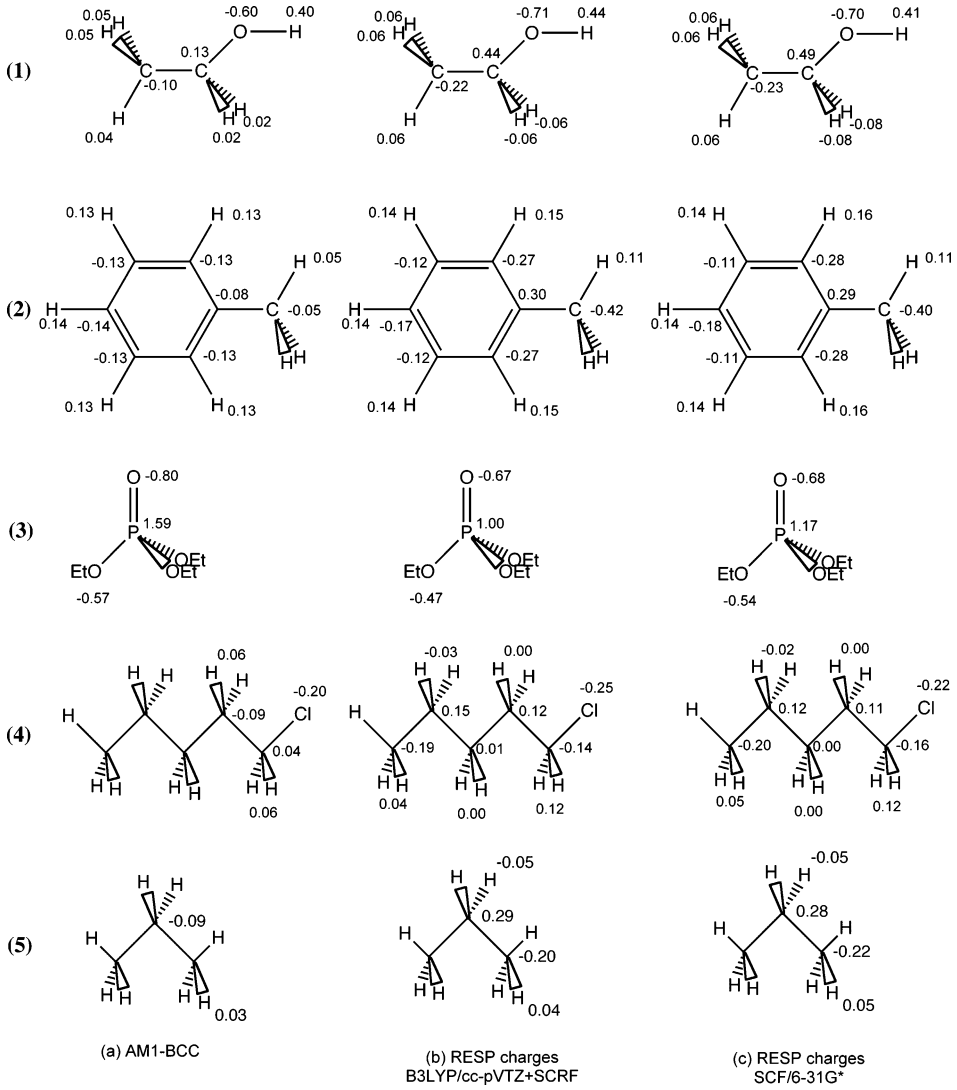

Figure 5. Sample partial charges for several small compounds, **1**−**5** show partial charges from (a) AM1-BCC and (b and c) RESP, from (b) B3LYP/cc-pVTZ+SCRF and (c) SCF/6-31G* electrostatic potentials. For these five compounds, ab initio charges are quite different from the empirical ones. The oxygen charge is more negative with ab initio methods, and the phosphorus atom seems difficult to describe accurately. For ethanol and 1-chloropentane, surprisingly, carbons were slightly positive and hydrogens were slightly negative, but the effect was relatively small.

is computationally much more expensive, so this relatively small difference in error highlights the virtue of implicit solvent. However, for some classes of molecules such as alcohols, there are significant differences for some charge models between explicit and implicit solvent (Table 3); for example, in implicit solvent, alcohols have an average unsigned error at least 0.6 kcal/mol worse, with RESP charges, than that in TIP3P water. This may be partly because implicit solvent fails to adequately treat the hydrogen bonding that is important for alcohols.

It is also worth pointing out, however, that implicit solvent models are fit, at least partly, to reproduce small-molecule hydration free energies. Even in two-term implicit solvent models, the nonpolar term is fit based on hydration free energies. Since there are only a limited number of such hydration free energies available, the comparison here may be biased in favor of implicit solvent (depending on how the solvent model was parametrized), since some of the small molecules studied here may be included in that fit. Furthermore, implicit solvent may perform quite differently for larger and less highly solvated molecules, such as proteins, so our observations may only have limited applicability.

G. Troublesome Chemical Classes. For alkanes, hydration free energies are essentially independent of the charges (cf. Figures 1 and 2 and the Supporting Information). However, the partial charges are quite different. For example, for methane, the carbon atomic charge is found to be −0.11 a.u. with the AM1-BCC method vs −0.47 a.u. with our best RESP approach (from a MP2/cc-pVTZ+SCRF electrostatic potential). This may be an instance of an instability in ESP-derived buried charges that persists in RESP,[18] since the dipole moment for both sets of charges is still zero.

The error for alkanes cannot be attributed solely to the GAFF parameters, since the hydration free energies are substantially different depending on the choice of water model, while the Lennard-Jones and bonded parameters for the molecules in our test set remain the same. Thus, the water model is the likely source of error, suggesting that alkane hydration free energies could be useful in developing reliable water models, when combined with other criteria already proposed.[58] There have already been some efforts in this direction.[59]

For alcohols, RESP charges seem to improve agreement with experimental results compared to empirical charges, as shown in the last column of Table 3. Additionally, for the majority of the compounds in our test set, the partial charges strongly influence the computed hydration free energies. The difference is generally larger for highly polar compounds and can be as

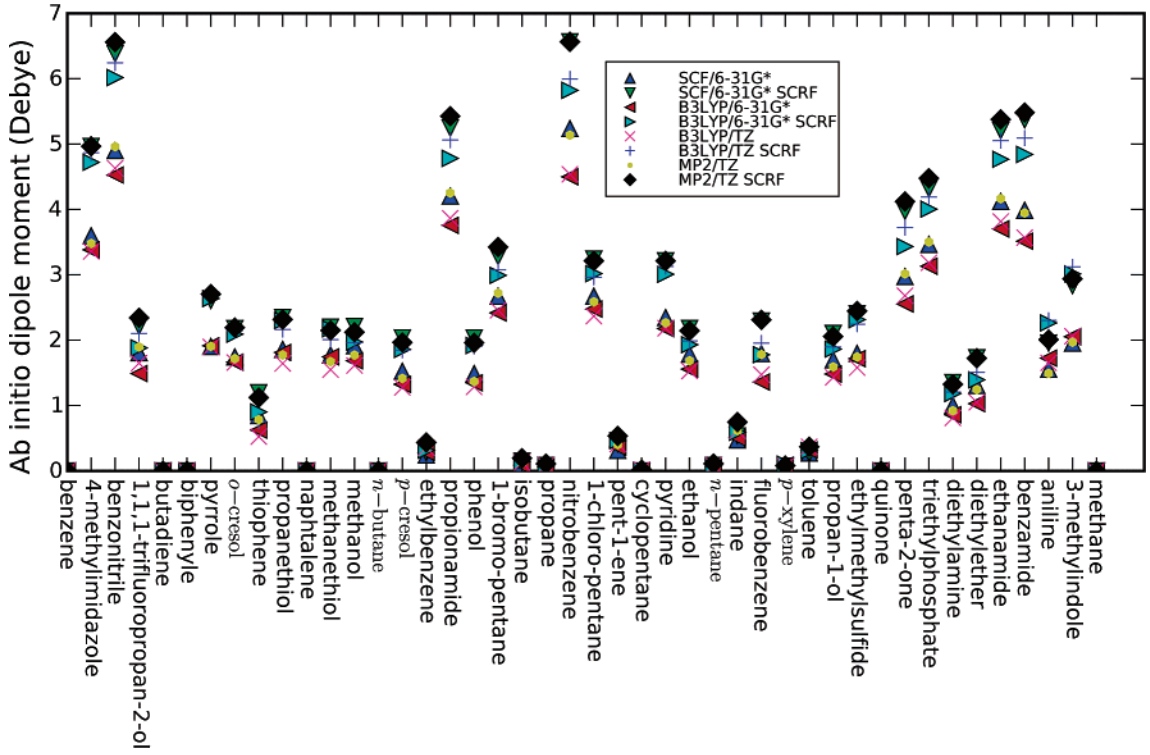

Figure 6. Variation in ab initio dipole moment across levels of theory. The ab initio dipole moment is sensitive to the level of the quantum calculation and especially to the difference between vacuum and reaction field treatments, as might be expected.

TABLE 3: Influence of Water Model on Hydration Free Energy Errors

water model	charge model	all compounds	subset by functionalities		
			alkanes (6)	arenes (6)	alcohols (6)
implicit[25]	AM1BCC	1.35	0.26	0.29	1.41
	AMSOL	2.46	0.31	1.34	2.08
	RESP (SCF/6-31G*)	1.28	0.49	0.23	2.00
explicit TIP3P	AM1BCC	0.92	0.51	0.30	1.43
	AMSOL	1.38	0.41	0.73	1.49
	RESP (SCF/6-31G*)	0.82	0.47	1.05	0.84
	RESP (B3LYP/cc-pVTZ+SCRF)	0.78	0.47	0.60	0.46
explicit TIP4P-Ew	AM1 BCC	1.24	1.09	0.75	1.06
	AMSOL	1.55	1.09	0.99	1.41
	RESP (SCF/6-31G*)	1.27	0.89	0.85	1.41
	RESP (B3LYP/cc-pVTZ+SCRF)	1.45	0.87	1.08	1.04

[a] The average unsigned errors (AUEs) for several charge sets are shown. These were computed from our data and are compared to results for the same set of compounds in implicit solvent from the work of Rizzo et al.[25] (data provided by R. Rizzo). Overall results are compared as well as several subfamilies of compounds. Values are given in kcal/mol.

much as a factor of 2 for molecules such as amides, triethylphosphate, and 4-methylimidazole. Indeed, the variation in computed hydration free energies is strongly correlated with the magnitude of the hydration free energy, as shown in Figure 3.

These compounds that are strongly influenced by the partial charges often involve highly ionic bonds that are more difficult to describe than C−H bonds. For example, the phosphorus atom in triethylphosphate, which is bonded to three oxygens, has a charge ranging from 0.90 to 1.19 a.u. for the eight RESP charge sets, whereas empirical methods give 1.59 a.u. for AM1-BCC and 2.26 a.u. for AM1-CM2. This seems to result in an overestimate of the hydration free energy of triethylphosphate with the semiempirical charges.

Similarly, the charges for the O═C−N sequence of amides are quite different across the charge sets. The nitrogen partial charge varies from −0.68 a.u. (AM1-BCC) to −1.05 a.u. (RESP with MP2/cc-pVTZ+SCRF).

H. Dipole Moments. RESP was designed to accurately fit the electrostatic potential resulting from a quantum calculation, meaning that it should reproduce the dipole moment of the quantum mechanical charge distribution well. We compare ab initio and RESP dipole moments in Figure 7 and find that this is indeed the case. However, there is substantial variation in dipole moment across theory levels (Figure 6). This, coupled with the strong correlation between computed hydration free energy and dipole moment (independent of charge model), suggests that a significant part of the error in computed hydration free energies may be the failure to correctly predict the appropriate dipole and multipole moments for these molecules.

I. Agreement as a Function of Theory Level. It is also interesting to note that our results do not substantially improve with increasing levels of quantum theory. This suggests that there may be some other source of error that dominates the observed discrepancy with experiment. Part of this may be the dipole moment, which varies across QM level, as discussed

TABLE 4: Comparison of Experimental with Computed Hydration Free Energies That Include an Estimate of Polarizing the Electronic Charge Distribution from the Gas to the Condensed Phase, Computed from the B3LYP/cc-pVTZ Quantum Chemical Calculations with and without a SCRF[a]

		SCF/6-31G*	SCF/6-31G* SCRF	B3LYP/6-31G*	B3LYP/6-31G* SCRF	B3LYP/TZ	B3LYP/TZ SCRF	MP2/TZ	MP2/TZ SCRF
TIP4P-Ew	AUE	1.55	1.73	2.76	1.41	2.67	1.41	1.85	1.88
	RMSE	1.89	2.67	3.24	1.86	3.18	1.69	2.26	3.09
	R^2	0.90	0.92	0.85	0.92	0.85	0.92	0.84	0.90
	slope	0.93	1.42	0.72	1.23	0.73	1.14	0.89	1.47
TIP3P	AUE	1.43	0.93	2.48	0.85	2.43	0.92	1.65	1.02
	RMSE	1.83	1.26	2.96	1.04	2.91	1.13	2.10	1.44
	R^2	0.94	0.97	0.93	0.96	0.94	0.97	0.91	0.95
	slope	0.81	1.16	0.66	1.03	0.66	0.96	0.77	1.17

[a] Values are given in kcal/mol. We report average unsigned errors (AUEs), root-mean-square error (RMSEs), linear correlation coefficients (R^2), and the slopes of this correlation between experimental and calculated hydration free energies.

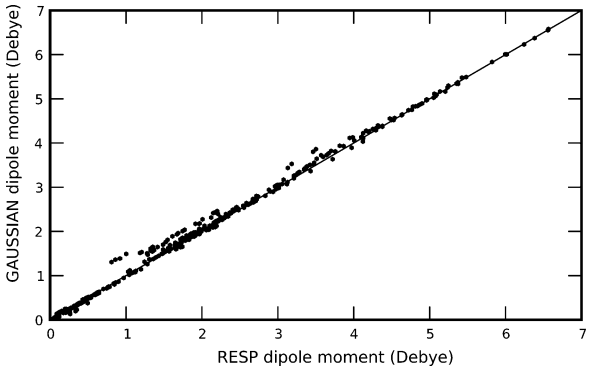

Figure 7. Comparison of ab initio and RESP-derived dipole moments. Dipole moments computed from RESP-derived partial atomic charges are compared with those computed directly from the electronic wave function from ab initio calculations ($R^2 = 1.00$, slope $= 1.01$).

TABLE 5: Statistics for Corrected SCRF Hydration Free Energies That Include the Quantum Mechanical Energy Cost of Polarizing the Charge Distribution from the Vacuum Distribution to That Computed Using SCRF[a]

		SCF/6-31G* SCRF	B3LYP/6-31G* SCRF	B3LYP/TZ SCRF	MP2/TZ SCRF
TIP4P-Ew	AUE	1.78	1.44	1.41	1.85
	RMSE	2.74	1.92	1.69	3.03
	R^2	0.90	0.89	0.89	0.88
	slope	1.52	1.30	1.16	1.54
TIP3P	AUE	0.97	0.82	0.92	0.99
	RMSE	1.31	1.00	1.13	1.38
	R^2	0.95	0.95	0.95	0.94
	slope	1.21	1.06	0.95	1.19

[a] The computed errors are not significantly better than those in Table 1, although they are more consistent across the levels of theory.

above. Part of it may also be the water model, as discussed above. However, Lennard-Jones parameters seem to be a significant possibility as well, since these will undoubtedly have a strong influence on hydration free energies. At the very least, Lennard-Jones parameters represent a second set of parameters that could be modified, in addition to the charges. The fact that our results do not improve substantially when higher levels of theory are used to compute partial charges may suggest that the dominant source of error is actually the Lennard-Jones parameters or possibly the lack of polarizability.

J. Polarization Corrections. We find that the two types of polarization corrections that we applied (see section II.F) did not lead to significant improvement in the agreement between our computed hydration free energies and experimental results. One of these two approaches (the approach of correcting hydration free energies computed using a continuum treatment of solvent using an estimate of the energy cost of polarizing the molecule), however, does significantly improve the consistency of results across different levels of quantum theory, which is, indeed, desirable.

Results are shown in Tables 4 and 5. It is also worth noting that these corrections can be very large, up to several kcal/mol for some compounds (Supporting Information). Similar corrections have been noted previously.[15] This is very large compared to experimental uncertainties of approximately 0.2 kcal/mol, and thus it may not be wise to ignore these contributions. It also may not be wise to parametrize force fields to reproduce hydration free energies without including the effects of polarization. The fact that inclusion of the correction improves agreement across theory levels suggests that it may be important to include this contribution generally; otherwise computed free energies may be unreasonably sensitive to the partial charges used.

IV. Conclusions

We have tested various approaches for obtaining partial charges for computing hydration free energies of small molecules using alchemical absolute free energy methods. These calculations lead to a number of main conclusions.

First, on the basis of comparison with the similar tests of Rizzo et al.,[25] implicit solvent performs nearly as well as explicit solvent for hydration free energies (with the notable exception of alcohols).

Second, improving the level of quantum theory used for calculating the electrostatic potential for charge fitting does not substantially improve the hydration free energies, implying that a main source of error in these calculations lies elsewhere, probably in the Lennard-Jones parameters and water model, although polarization is a significant possibility. Our computed hydration free energies here provide a benchmark with which to compare improved models/force fields, such as polarizable force fields and improved Lennard-Jones parameters or water models.

Third, our results strongly suggest that, with current charge models and force fields, hydration free energies cannot be computed to accuracies better than roughly 1 kcal/mol on average, suggesting that binding free energies probably also cannot reliably be computed with accuracies greater than 1 kcal/mol, except in special cases (for example, if ligands are very nonpolar and so accuracies are better or if errors fortuitously cancel).

At present, AM1-BCC semiempirical charges perform essentially as well for hydration free energies as any of the other methods, with significantly less computational expense. This may be because AM1-BCC charges are very similar to the SCF/6-31G* RESP charges, which were used in parametrizing the force field. Unless there is some compelling reason to use another charge set in drug discovery calculations (such as the desire to use an implicit solvent model that has been parametrized for use with a particular charge model) the AM1-BCC and SCF/6-31G* charge sets appear to be a good general-purpose choice, at least with the force field considered here, when judged by hydration free energies. However, it is worth remembering that AM1-BCC charges cannot be expected to perform well outside of the chemical space used in their parametrization.

In addition, we find that TIP3P water works slightly better for hydration free energies than TIP4P-Ew. Finally, not surprisingly, computed hydration free energies grow substantially worse (and vary more across levels of quantum theory) with increasing polarity of the compound being considered. Calculated dipole moments are also fairly dependent on the method used to calculate the electrostatic potential for charge fitting, and this variation may be the origin of some of the variation across theory levels.

In view of the results presented here, it seems likely that, to achieve accuracies significantly below the roughly 1 kcal/mol RMSE seen here, it will become necessary to not only develop improved water models but also revisit the Lennard-Jones parameters and test whether improving these in conjunction with improving the partial charges can improve hydration free energies. This approach does, however, have one major conceptual drawback: It is not entirely clear, in view of the neglect of polarization effects in fixed-charge force fields, how parameters should be developed that can simultaneously be appropriate in the many various different solvent and protein environments common in molecular simulation. Additionally, as discussed above, it is difficult to know how to adjust hydration free energies for the effect of polarizing the charge distribution when a molecule is transferred from vacuum to water. It is somewhat more clear how to consistently treat polarization effects when using polarizable force fields.[14] Therefore, we are working on extending this work to compute hydration free energies for small molecules using polarizable force fields.

While further development of fixed-charge force fields may hold promise, it may be that an average error of roughly 1 kcal/mol is approaching the fundamental limit of these force fields. Comparison of the results presented here with those from improved and/or polarizable force fields will help to answer this question.

Acknowledgment. The authors thank William C. Swope, Jed W. Pitera, Julia E. Rice (IBM Almaden Research Center), Terry Lang (UCSF), Christopher Bayly (Merck Frosst), Michael Shirts (Columbia), and Vijay Pande (Stanford) for insightful discussion relating to this work as well as Libusha Kelly, Matt Jacobson (UCSF), and Chris Oostenbrink (Vrije Universiteit, Amsterdam) for critical comments on this manuscript. We thank Eric J. Sorin and Vijay S. Pande (Stanford) for providing the AMBER-to-GROMACS conversion script used to convert ligand parameters and Kaushik Raha (UCSF) for providing AM1-BCC charges. We thank Robert C. Rizzo for providing access to his data that was used in generating Table 3. E.D. gratefully acknowledges a graduate fellowship from the French Research Minister. J.D.C. was supported in part by Howard Hughes Medical Institute and IBM predoctoral fellowships. D.L.M. and K.A.D. acknowledge the National Institutes of Health (Grant No. GM63592), Anteon Corporation (Grant No. USAF-5408-04-SC-0008,) and a UCSF Sandler Award for financial support. This work was performed in part with the UCSF QB3 Shared Computing Facility. Quantum chemical calculations were performed on CCR clusters (University Paris VI).

Supporting Information Available: Table of calculated and experimental hydration free energies for each molecule, method, and water model in the test set; optimized geometries of all of the molecules in the test set; Lennard-Jones components of the hydration free energies; polarization energies; equivalents to Figures 1−3 and 5 for TIP4P-Ew; and correlation of the electrostatic component of the hydration free energy with the dipole moment. This material is available free of charge via the Internet at http://pubs.acs.org.

References and Notes

(1) Shoichet, B. K.; Leach, A. R.; Kuntz, I. D. *Proteins: Struct., Funct., Genet.* **1999**, *34*, 4−16.
(2) Kalyanaraman, C.; Bernacki, K.; Jacobson, M. P. *Biochemistry* **2005**, *44*, 2059−2071.
(3) Camacho, C. J.; Ma, H.; Champ, P. C. *Proteins: Struct., Funct., Bioinf.* **2006**, *63*, 868−877.
(4) Ferrara, P.; Gohlke, H.; Price, D. J.; Klebe, G.; Brooks, C. L., III. *J. Med. Chem.* **2004**, *47*, 3032−3047.
(5) Huang, N.; Kalyanaraman, C.; Jacobson, M. P. *J. Chem. Inf. Model.* **2006**, *46*, 243−253.
(6) Shirts, M. R.; Pitera, J. W.; Swope, W. C.; Pande, V. S. *J. Chem. Phys.* **2003**, *119*, 5740−5761.
(7) Shirts, M. R.; Pande, V. S. *J. Chem. Phys.* **2005**, *122*, 134508.
(8) Wang, J.; Wolf, R. M.; Caldwell, J. W.; Kollman, P. A.; Case, D. A. *J. Comput. Chem.* **2004**, *25*, 1157−1174.
(9) Ponder, J. W.; Case, D. A. *Adv. Protein Chem.* **2003**, *66*, 27−85.
(10) Wang, J.; Wang, W.; Kollman, P. A.; Case, D. A. *J. Mol. Graphics Modell.* **2006**, *26*, 247260.
(11) Chambers, C. C.; Hawkins, G. D.; Cramer, C. J.; Truhlar, D. G. *J. Phys. Chem. A* **1996**, *100*, 16385−16398.
(12) Hawkins, G. D.; Cramer, C. J.; Truhlar, D. G. *J. Phys. Chem. B* **1998**, *102*, 3257−3271.
(13) Duan, Y.; Wu, C.; Chowdhury, S.; Lee, M. C.; Xiong, G.; Zhang, W.; Yang, R.; Cieplak, P.; Luo, R.; Lee, T.; Caldwell, J.; Wang, J.; Kollman, P. *J. Comput. Chem.* **2003**, *105*, 2999−3094.
(14) Ren, P.; Ponder, J. W. *J. Comput. Chem.* **2002**, *123*, 1497−1506.
(15) Chipot, C. *J. Comput. Chem.* **2003**, *24*, 409−415.
(16) Hess, B.; van der Vegt, N. F. A. *J. Phys. Chem. B* **2006**, *110*, 17616−17626.
(17) Li, J. B.; Zhu, T. H.; Cramer, C. J.; Truhlar, D. J. *J. Phys. Chem. A* **1998**, *102*, 1820−1831.
(18) Jakalian, A.; Bush, B. L.; Jack, D. B.; Bayly, C. I. *J. Comput. Chem.* **2000**, *21*, 132−146.
(19) Bayly, C. I.; Cieplak, P.; Cornell, W. D.; Kollman, P. A. *J. Phys. Chem.* **1993**, *97*, 10269−10280.
(20) Jorgensen, W. L.; Chandrasekhar, J.; Madura, J. D.; Impey, R.W.; Klein, M. L. *J. Chem. Phys* **1983**, *79*, 926−935.
(21) Horn, H. W.; Swope, W. C.; Pitera, J. W.; Madura, J. D.; Dick, T. J.; Hura, G. L.; Head-Gordon, T. *J. Chem. Phys.* **2004**, *120*, 9665−9678.
(22) Kastenholz, M. A.; Hünenberger, P. H. *J. Chem. Phys.* **2006**, *124*, 224501.
(23) Frisch, M. J.; Trucks, G. W.; Schlegel, H. B.; Scuseria, G. E.; Robb, M. A.; Cheeseman, J. R.; Montgomery, J. A., Jr.; Vreven, T.; Kudin, K. N.; Burant, J. C.; Millam, J. M.; Iyengar, S. S.; Tomasi, J.; Barone, V.; Mennucci, B.; Cossi, M.; Scalmani, G.; Rega, N.; Petersson, G. A.; Nakatsuji, H.; Hada, M.; Ehara, M.; Toyota, K.; Fukuda, R.; Hasegawa, J.; Ishida, M.; Nakajima, T.; Honda, Y.; Kitao, O.; Nakai, H.; Klene, M.; Li, X.; Knox, J. E.; Hratchian, H. P.; Cross, J. B.; Bakken, V.; Adamo, C.; Jaramillo, J.; Gomperts, R.; Stratmann, R. E.; Yazyev, O.; Austin, A. J.; Cammi, R.; Pomelli, C.; Ochterski, J. W.; Ayala, P. Y.; Morokuma, K.; Voth, G. A.; Salvador, P.; Dannenberg, J. J.; Zakrzewski, V. G.; Dapprich, S.; Daniels, A. D.; Strain, M. C.; Farkas, O.; Malick, D. K.; Rabuck, A. D.; Raghavachari, K.; Foresman, J. B.; Ortiz, J. V.; Cui, Q.; Baboul, A. G.; Clifford, S.; Cioslowski, J.; Stefanov, B. B.; Liu, G.; Liashenko, A.; Piskorz, P.; Komaromi, I.; Martin, R. L.; Fox, D. J.; Keith, T.; Al-Laham, M. A.; Peng, C. Y.; Nanayakkara, A.; Challacombe, M.; Gill, P. M. W.;

Johnson, B.; Chen, W.; Wong, M. W.; Gonzalez, C.; Pople, J. A. *Gaussian 03*, revision C.02; Gaussian, Inc.: Wallingford, CT, 2004.

(24) Bordner, A. J.; Cavasotto, C. N.; Abagyan, R. A. *J. Phys. Chem. B* **2002**, *106*, 11009−11015.

(25) Rizzo, R. C.; Aynechi, T.; Case, D. A.; Kuntz, I. D. *J. Chem. Theory Comput.* **2006**, *2*, 128−139.

(26) Becke, A. D. *J. Chem. Phys.* **1993**, *98*, 5648−5652.

(27) Lee, C.; Yang, W.; Parr, R. G. *Phys. Rev. B* **1988**, *37*, 785−789.

(28) Dunning, T. H. *J. Chem. Phys.* **1971**, *55*, 716−723.

(29) Koch, W.; Holthausen, M. C. *A Chemist's Guide to Density Functional Theory*, 2nd ed.; Wiley: New York, 2001.

(30) Moller, C.; Plesset, M. S. *Phys. Rev.* **1934**, *46*, 618−622.

(31) Hariharan, P. C.; Pople, J. A. *Theor. Chim. Acta* **1973**, *28*, 213.

(32) Case, D. A.; Darden, T. A.; Cheatham, T. E., III.; Simmerling, C. L.; Wang, J.; Duke, R. E.; Luo, R.; Merz, K. M.; Wang, B.; Pearlman, D. A.; Crowley, M.; Brozell, S.; Tsui, V; Gohlke, H.; Mongan, J.; Hornak, V.; Cui, G.; Beroza, P.; Schafmeister, C.; Caldwell, J. W.; Ross, W. S.; Kollman, P. A. *AMBER 8 User's Manual*; University of California: San Francisco, 2004.

(33) Felder, C.; Jiang, H.-L.; Zhu, W.-L.; Chen, K.-X.; Silman, I.; Botti, S. A.; Sussman, J. L. *J. Phys. Chem. A* **2001**, *105*, 1326−1333.

(34) Patel, S.; Mackerrell, A. D., Jr.; Brooks, C. L., III. *J. Comput. Chem.* **2004**, *25*, 1504−1514.

(35) Tomasi, J.; Mennucci, B.; Cammi, R. *Chem. Rev.* **2005**, *105*, 2999−3094.

(36) Wiberg, K. B.; Rablen, P. R. *J. Comput. Chem.* **1993**, *14*, 1504−1518.

(37) Stouch, T. R.; Williams, D. E. *J. Comput. Chem.* **1992**, *12*, 622−632.

(38) Dupradeau, F.-Y.; Pigache, A.; Zaffran, T.; Cieplak, P. *R.E.D. Version 2.0 User's Manual and Tutorial*; Université de Picardie Jules Verne: Amiens, France, 2005. http://www.u-picardie.fr/labo/lbpd/RED/RED-II.pdf.

(39) Hawkins, G. D.; Giesen, D. J.; Lynch, G. C.; Chambers, C. C.; Rossi, I.; Storer, J. W.; Li, J.; Zhu, T.; Thompson, J. D.; Winget, P.; Lynch, B. J.; Rinaldi, D.; Liotard, D. A.; Cramer, C. J.; Truhlar, D. G. *AMSOL*, version 6.5.3; University of Minnesota: Minneapolis, MN, 1998. http://comp.chem.umn.edu/amsol/.

(40) Case, D. A.; Darden, T. A.; Cheatham, T. E., III.; Simmerling, C. L.; Wang, J.; Duke, R. E.; Luo, R.; Merz, K. M.; Wang, B.; Pearlman, D. A.; Crowley, M.; Brozell, S.; Tsui, V; Gohlke, H.; Mongan, J.; Hornak, V.; Cui, G.; Beroza, P.; Schafmeister, C.; Caldwell, J. W.; Ross, W. S.; Kollman, P. A. *AMBER*, version 8; University of California: San Francisco, 2004.

(41) The AMBER-to-GROMACS conversion script was originally written by Eric Sorin in the laboratory of Vijay Pande and modified and updated by the present authors. It is available online at http://folding.stanford.edu/ffamber.

(42) Bennett, C. H. *J. Comput. Phys.* **1976**, *22*, 245−268.

(43) Shirts, M. R.; Bair, E.; Hooker, G.; Pande, V. S. *Phys. Rev. Lett.* **2003**, *91*, 140601.

(44) Zwanzig, R. W. *J. Chem. Phys.* **1954**, *22*, 1420.

(45) Mobley, D. L.; Chodera, J. D.; Dill, K. A. *J. Chem. Phys.* **2006**, *125*, 084902.

(46) Lindahl, E.; Hess, B.; van der Spoel, D. *J. Mol. Model.* **2001**, *7*, 306−317.

(47) van der Spoel, D.; Lindahl, E.; Hess, B.; Groenhof, G.; Mark, A. E.; Berendsen, H. J. C. *J. Comput. Chem.* **2005**, *26*, 1701−1718.

(48) Essmann, U.; Perera, L.; Berkowitz, M. L.; Darden, T.; Lee, H.; Pedersen, L. G. *J. Chem. Phys.* **1995**, *103*, 8577−8593.

(49) van Gunsteren, W. F.; Berendsen, H. J. C. *Mol. Simul.* **1988**, *1*, 173−185.

(50) Liu, D. C.; Nocedal, J. *Math. Program., Ser. B* **1989**, *45*, 503−528.

(51) Berendsen, H. J. C.; Postma, J. P. M.; van Gunsteren, W. F.; DiNola, A.; Haak, J. R. *J. Chem. Phys.* **1984**, *81*, 3584−3690.

(52) Hess, B.; Bekker, H.; Berendsen, H. J. C. *J. Comput. Chem.* **1997**, *18*, 1463−1472.

(53) Carlstin, E. *Ann. Statist.* **1986**, *14*, 1171−1179.

(54) Janke, W. Statistical analysis of simulations: Data correlations and error estimation. In *Quantum Simulations of Complex Many-Body Systems: From Theory to Algorithms*; Grostendorst, J.; Marx, D.; Murmatsu, A., Eds.; John von Neumann Institute for Computing: Julich, Germany, 2002.

(55) Chodera, J. D.; Swope, W. C.; Pitera, J. W.; Seok, C.; Dill, K. A. *J. Chem. Theor. Comput.* **2007**, *3*, 26−41.

(56) Pylasunov, A. V.; Shock, E. L. *Geochim. Cosmochim. Acta* **2000**, *64*, 439−468.

(57) Abraham, M. H.; Whiting, G. S. *J. Chem. Soc., Perkin Trans. 2* **1990**, 291−300.

(58) Guillot, B. *J. Mol. Liq.* **2002**, *101*, 219−260.

(59) Oostenbrink, C.; Villa, A.; Mark, A. E.; Gunsteren, W. F. V. *J. Comput. Chem.* **2004**, *25*, 1656−1676.

(60) The AMBER 8 version of ANTECHAMBER omits improper torsions for some molecules for which improper torsions are included in some later versions of ANTECHAMBER. Hence, there may be some systematic differences in the parameters generated with this version of ANTECHAMBER compared to those generated with some later versions. These improper torsions typically seem to involve aromatic hydrogens and carbons in molecules such as phenol and *o*-cresol and enforce hydrogen planarity. We have tested the robustness of our results to these parameters by repeating our calculations for several molecules (phenol and *o*-cresol) with parameters generated using ANTECHAMBER version 1.2.4 and found that any differences in computed hydration free energies were within the statistical uncertainty; hence we have not further examined this issue here.

(61) We are suspicious that the block bootstrap method used here underestimates the true uncertainty by some small factor, as repeated calculations of the hydration free energy for several small molecules using the protocol reported here led to standard deviations that were larger than the computed uncertainties in the individual calculations by perhaps a factor of 3. This issue will be explored in detail elsewhere. Regardless, the block bootstrap method used here seems to be the best we can do at present, since the error analysis developed so far for the BAR method neglects time correlations[43] in the data and thus also represents an underestimate of the true uncertainty.